BJP British Journal of Pharmacology

DOI:10.1111/bph.12932
www.brjpharmacol.org

RESEARCH PAPER

Effect of erythropoietin on hepatic cytochrome P450 expression and function in an adenine-fed rat model of chronic kidney disease

D A Feere[1], T J Velenosi[1] and B L Urquhart[1,2,3]

Departments of [1]Physiology and Pharmacology, and [3]Medicine, Schulich School of Medicine and Dentistry, Western University, London, ON, Canada, and [2]Lawson Health Research Institute, London, ON, Canada

Correspondence
Bradley L Urquhart, 1151 Richmond Street, Dental Sciences Building Room 2011, London, Ontario, Canada N6A 5C1.
E-mail:
Brad.Urquhart@schulich.uwo.ca

Received
9 January 2014
Revised
4 September 2014
Accepted
8 September 2014

BACKGROUND AND PURPOSE

Erythropoietin (EPO) is used to treat anaemia associated with chronic kidney disease (CKD). Hypoxia is associated with anaemia and is known to cause a decrease in cytochrome P450 (P450) expression. As EPO production is regulated by hypoxia, we investigated the role of EPO on P450 expression and function.

EXPERIMENTAL APPROACH

Male Wistar rats were subjected to a 0.7% adenine diet for 4 weeks to induce CKD. The diet continued for an additional 2 weeks while rats received EPO by i.p. injection every other day. Following euthanasia, hepatic P450 mRNA and protein expression were determined. Hepatic enzyme activity of selected P450s was determined and chromatin immunoprecipitation was used to characterize binding of nuclear receptors involved in the transcriptional regulation of CYP2C and CYP3A.

KEY RESULTS

EPO administration decreased hepatic mRNA and protein expression of CYP3A2 ($P < 0.05$), but not CYP2C11. Similarly, EPO administration decreased CYP3A2 protein expression by 81% ($P < 0.001$). A 32% decrease ($P < 0.05$) in hepatic CYP3A enzymatic activity (V_{max}) was observed for the formation of 6βOH-testosterone in the EPO-treated group. Decreases in RNA pol II recruitment ($P < 0.01$), hepatocyte nuclear factor 4α binding ($P < 0.05$) and pregnane X receptor binding ($P < 0.01$) to the promoter region of CYP3A were also observed in EPO-treated rats.

CONCLUSIONS AND IMPLICATIONS

Our data show that EPO decreases the expression and function of CYP3A, but not CYP2C in rat liver.

Abbreviations

AhR, aryl hydrocarbon receptor; ALT, alanine transaminase; AST, aspartate transaminase; CAR, constitutive androstane receptor; CKD, chronic kidney disease; EPO, erythropoietin; H&E, haematoxylin and eosin; HIF, hypoxia-inducible factor; HNF-4α, hepatocyte nuclear factor 4α; JAK2, Janus kinase 2; LXR, liver X receptor; P450, cytochrome P450; PXR, pregnane X receptor; RXRα, retinoid X receptor α; STAT5, signal transducer and activator of transcription 5

Tables of Links

TARGETS	
Enzymes[a]	**Nuclear receptors**[b]
CYP1A2	CAR, constitutive androstane receptor
CYP2C	HNF-4α, hepatocyte nuclear factor 4α
CYP2D6	LXR, liver X receptor
CYP3A2	PXR, pregnane X receptor
JAK2, Janus kinase 2	RXRα, retinoid X receptor α

LIGANDS
Adenine
Carbamazepine
EPO, erythropoietin
Flurazepam
Midazolam
Testosterone

These Tables list key protein targets and ligands in this article which are hyperlinked to corresponding entries in http://www.guidetopharmacology.org, the common portal for data from the IUPHAR/BPS Guide to PHARMACOLOGY (Pawson *et al.*, 2014) and are permanently archived in the Concise Guide to PHARMACOLOGY 2013/14 ([a,b]Alexander *et al.*, 2013a,b).

Introduction

Chronic kidney disease (CKD) is a progressive, irreversible loss of renal function characterized by decreasing glomerular filtration rate. Rates of CKD in the population are increasing, largely because of increasing prevalence of associated comorbidities such as diabetes and hypertension. Patients with CKD are commonly prescribed more than seven drugs concurrently, with even higher prescription rates among dialysis patients, to manage their CKD and comorbidities (Talbert, 1994; Manley *et al.*, 2004). Drug dosing in CKD is complicated by altered pharmacokinetic profiles, involving reduced renal and non-renal clearance of drugs (Velenosi and Urquhart, 2014). These pharmacokinetic alterations and the heavy medication burden result in high rates of adverse drug events in patients with CKD (Manley *et al.*, 2004; Nolin *et al.*, 2009). Accordingly, the US Food and Drug Administration has published recommendations for evaluation of drug pharmacokinetics, dosing and labelling in patients with renal impairment (FDA, 2010).

Non-renal clearance of most drugs largely involves drug metabolism. In fact, the majority of prescribed drugs require some degree of metabolism prior to elimination from the body. The primary site of drug metabolism is the liver, and these reactions are primarily mediated by cytochrome P450 (P450) enzymes (Wienkers and Heath, 2005). CYP3A4/5 is responsible for the metabolism of 30–50% of all clinically used drugs with the CYP2C subfamily accounting for metabolism of approximately 24% of drugs. (Wrighton *et al.*, 1996; Nolin *et al.*, 2003; Zanger and Schwab, 2013). Previous studies using animal models of moderate and severe CKD have shown decreased hepatic expression and function of CYP2C, the most abundant P450 in rat liver, and CYP3A (Leblond *et al.*, 2000; 2001; Velenosi *et al.*, 2012).

Erythropoietin (EPO) is a glycoprotein hormone produced by the interstitial cells of the kidney (Lacombe *et al.*, 1988). Normally produced by the healthy kidney in response to hypoxia, the primary action of EPO is to control proliferation and differentiation of erythroid progenitor cells. Accordingly, EPO is commonly used to treat anaemia associated with CKD and is also used in the treatment of other anaemia-related disorders such as those encountered during chemotherapy, treatment of HIV and rheumatic disease. Specific to CKD, haemodialysis patients require doses of recombinant human EPO three times per week to maintain blood haematocrit required for sufficient tissue oxygenation (Eschbach, 2002).

Although investigated for decades in the regulation of red blood cell production, other non-haematopoietic roles of EPO have been recently discovered. The non-haematopoietic effects of EPO signalling have been largely investigated in the protection of cells from ischemia and reperfusion injury in the CNS, heart, kidney and liver. The direct effects of EPO are mediated by interaction at the surface of cells, including hepatocytes, that express the EPO receptor (Pinto *et al.*, 2008). Further, recent evidence also suggests that EPO-mediated signalling is able to activate hepatic transcription factors including the nuclear receptor liver X receptor (LXR; Pinto *et al.*, 2008; Lu *et al.*, 2010). Nuclear receptor activation by EPO is of particular interest as enzymes and transporters involved in drug metabolism and disposition are transcriptionally regulated by xenosensing nuclear receptors. Specifically, CYP3A4 expression is regulated by pregnane X receptor (PXR), and both CYP3A and CYP2C enzymes are regulated by hepatocyte nuclear factor 4α (HNF-4α; Ibeanu and Goldstein, 1995; Tirona *et al.*, 2003). Despite these findings and the increasing number of CKD patients receiving EPO to treat anaemia, the effect of continuous EPO administration on the enzymes involved in drug metabolism in the presence, or absence, of CKD has not been directly investigated.

The objective of this study was to examine the effect of EPO on P450 expression and function in the presence, and absence, of CKD. We utilized an adenine-fed rat model of CKD combined with treatment of recombinant human EPO to evaluate its effects on hepatic expression and activity of CYP2C and CYP3A drug-metabolizing enzymes. We hypothesized that the treatment with EPO would partly restore CKD-mediated down-regulation of P450 expression and activity.

Methods

Experimental model

All animal care and experimental protocols and procedures were approved by the Western University Animal Care Com-

mittee and conducted in accordance with the Canadian Council on Animal Care. Studies involving animals are reported in accordance with the ARRIVE guidelines for reporting experiments involving animals (Kilkenny *et al.*, 2010; McGrath *et al.*, 2010). A total of 32 animals were used in the experiments described here.

Male Wistar rats, 6 weeks of age (weighing 150 g), were obtained from Charles River Laboratories, Inc. (Wilmington, MA, USA). Animals were acclimated for 4 days on a 12 h light cycle with standard rat chow and water *ad libitum*.

Adenine-induced CKD

After acclimation, rats were assigned to a normal chow diet (n = 16) or a chow diet supplemented with 0.7% adenine (n = 16) for 6 weeks. Rats were pair-fed, food was weighed daily and control rats were fed the same mass of food per day as their adenine-fed counterparts. After 4 weeks on the adenine or control diets, rats received either 150 U·kg^{-1} epoetin alfa, or saline, in a volume of 0.25 mL per 100 g body weight, by i.p. injection every other day for 2 weeks prior to euthanasia. The dose of EPO was selected to closely match the dose used in maintenance haemodialysis patients. The resulting treatments created four groups of equal number (n = 8) – chow-fed saline-injected rats (control), chow-fed EPO-injected rats (EPO), adenine-fed saline-injected rats (CKD) and adenine-fed EPO-injected rats (CKD EPO). After the 6 week protocol, rats were sacrificed under isoflurane anaesthesia by decapitation. Blood was collected and haematocrit, plasma markers of CKD (creatinine and urea) and liver enzymes [aspartate transaminase (AST) and alanine transaminase (ALT)] were determined by the London Laboratory Services group by standard methods (London, ON, Canada).

Histology

Fresh liver and kidney samples were fixed in 10% formalin obtained from Anachemia (Rouses Point, NY, USA). Tissue processing, sectioning and staining were completed by the Department of Pathology (Western University, Canada). Samples were dehydrated using ethanol, cleared with xylene and embedded in paraffin wax. Sections (5 µm) of the liver and kidney were cut, using a microtome, and mounted on slides before being rehydrated and stained with haematoxylin and eosin (H&E). Slides were visualized using an Olympus SZX16 microscope and Qcapture Pro software version 6.0 by QImaging (Redwood City, CA, USA).

Real-time PCR analysis

Hepatic total RNA was extracted using TRIzol Reagent from Life Technologies, Inc. (Burlington, ON, Canada) according to manufacturer's protocol. RNA concentration and quality were determined using a NanoDrop spectrophotometer from Thermo Scientific (West Palm Beach, FL, USA). cDNA was synthesized from 1 µg total RNA using qScript cDNA Supermix from Quanta Biosciences (Gaithersburg, MD, USA). Relative mRNA was quantified by real-time PCR with PerfeCta SYBR Green Fastmix from Quanta Biosciences (Gaithersburg, MD, USA). Specific primers were designed for CYP1A2, CYP2C11, CYP3A2, PXR, retinoid X receptor α (RXRα), constitutive androstane receptor (CAR), aryl hydrocarbon receptor (AhR) and HNF-4α using NCBI Primer-Blast. Gene expression was normalized to β-actin using the ΔΔCT method (Livak and Schmittgen, 2001). Relative mRNA levels were analysed compared with the control treatment group that received normal chow and saline injections.

Hepatic microsome isolation

Liver microsomes were isolated by differential centrifugation as described previously (Velenosi *et al.*, 2012). Liver tissue was rinsed in 0.9% NaCl solution and homogenized in 1.15% KCl containing 1 mM EDTA. Tissue homogenate was centrifuged at 9000 g for 20 min at 4°C. The resulting supernatant was centrifuged at 105 000 g for 60 min at 4°C. The microsome pellet was resuspended in 250 µL of 100 mM potassium phosphate buffer containing 20% glycerol at pH 7.4. Total protein concentration was quantified using Pierce BCA protein assay from Fisher Scientific (Waltham, MA, USA) and microsomes were aliquoted and stored at –80°C until use.

Determination of total P450 content

Microsomal protein was used to determine total P450 content using spectral analysis after reduction of P450 using carbon monoxide and sodium dithionite (Omura and Sato, 1964).

Western blot analysis

Microsomes were used for the determination of CYP1A, CYP2D, CYP2C11 and CYP3A2 protein expression using Western blot analysis. Twenty micrograms of microsomal protein were loaded per well in a 10% polyacrylamide gel containing 0.1% SDS and electrophoresed for 60 min at 120 V. Proteins were transferred to a nitrocellulose membrane for 60 min at 150 V and immunoblots were incubated at room temperature with primary antibodies for 90 min prior to being washed with PBS with 0.1% tween and incubated with secondary antibodies linked to HRP for 60 min. Primary antibodies used were polyclonal rabbit anti-rat CYP1A, dilution 1:5000, Detroit R&D, Inc. (Detroit, MI, USA), monoclonal mouse anti-rat CYP2C11, dilution 1:5000, Detroit R&D, Inc., polyclonal rabbit anti-rat CYP2D, dilution 1:5000, Detroit R&D, Inc., monoclonal rabbit anti-rat CYP3A2, dilution 1:10000, Millipore (Billerica, MA, USA), and monoclonal mouse anti-β-actin-peroxidase, dilution 1:50000, Sigma-Aldrich (St. Louis, MO, USA). HRP-linked secondary antibodies were purchased from Santa Cruz Biotechnology, Inc. (Santa Cruz, CA, USA). Luminata Forte Western HRP substrate was obtained from Millipore (Billerica, MA). Chemiluminescence from immune blots was imaged on a Bio-Rad VersaDoc Imaging System (Berkeley, CA, USA) and band intensity was quantified by densitometry using Bio-Rad Quantity One 1D analysis software.

Microsomal metabolism and analysis by ultra-performance liquid chromatography with photodiode array detection (UPLC-PDA) and LC/MS

Metabolic activity of CYP3A and CYP2C in hepatic microsomes was determined using probe substrates as previously described (Velenosi *et al.*, 2012). Full-enzyme kinetics was completed individually for each of the eight rats in the four treatment groups. Testosterone and midazolam were selected as substrates for CYP3A, and testosterone was used as a substrate for CYP2C activity. Testosterone metabolites 16αOH-testosterone and 6βOH-testosterone are formed by the

activity of CYP2C and CYP3A respectively. Buffered reactions, using 50 mM potassium phosphate with 2 mM $MgCl_2$ (pH 7.4), were conducted with 1 mg·mL^{-1} final hepatic microsomal protein concentration in a final volume of 250 µL. Metabolism was determined previously to be linear at 10 min for the formation of testosterone metabolites and 30 min for the formation of midazolam metabolites. All reactions were pre-incubated with probe substrates for 10 min at 37°C and initiated by the addition of 1 mM NADPH (final concentration). Substrate concentrations used were 50, 100, 400 and 1000 µM for testosterone and 5, 10, 30, 100 and 300 µM for midazolam. Reactions were terminated by adding 50 µL of ice-cold acetonitrile followed by 15 min incubation on ice and centrifugation at 20 000× *g* for 5 min to pellet precipitated protein. Metabolites of testosterone, 6βOH-testosterone (CYP3A) and 16αOH-testosterone (CYP2C), were extracted by solid-phase extraction, using carbamazepine as an internal standard, followed by UPLC-PDA as described previously (Velenosi *et al.*, 2012). Briefly, analytes were separated on a Kinetex 2.1 × 50 mm, 1.7 µm, C18 UPLC column, maintained at 40°C, using KH_2PO_4 (pH 3.0) and acetonitrile mobile phase. The isocratic conditions were 93:7 (KH_2PO_4 : acetonitrile) for 2 min followed by a 20:80 wash for 1 min prior to a 1 min re-equilibration at initial conditions. Detection of testosterone metabolites and carbamazepine was achieved measuring absorbance at 240 and 287 nm respectively. Concentrations were determined from standard curves generated for quantification of 6βOH-testosterone (0.1–25 µM) and 16αOH-testosterone (0.2–100.0 µM).

Quantification of midazolam metabolism was achieved using a Waters UPLC with a Waters Xevo G2-S Qtof mass spectrometer; 1-hydroxymidazolam and internal standard, flurazepam, were extracted using solid-phase extraction cartridges. Analytes were separated on a Waters Acquity BEH 2.1 × 50mm, 1.7 µm, C18 UPLC column, maintained at 40°C, using water with 0.01% formic acid (pump A) and acetonitrile (pump B) mobile phase. Linear gradient conditions were 20% B to 35% B over 2.5 min. The column was then washed with 80% B for 1 min prior to re-equilibration to initial conditions for an additional minute. The mass spectrometer was operated in positive electrospray ionization mode. An accurate m/z of 342.0889 [M-H$^+$] and 388.1592 [M-H$^+$] was used to detect 1-hydroxymidazolam and flurazepam respectively. Leucine-enkephalin (556.2771, [M-H$^+$]) was used as lockspray to ensure mass accuracy (<2 ppm) for all samples. Concentrations were determined from a standard curve generated for quantification of 1-hydroxymidazolam (0.1–100.0 µM).

Chromatin immunoprecipitation (ChIP)

ChIP was performed on rat liver tissue using previously published methods (Sohi *et al.*, 2011). In brief, tissue was homogenized and DNA cross-linked by 1% formaldehyde before being sheared by sonication. Sonicated chromatin was diluted, aliquoted and stored at –80°C. Samples were precleared with protein A/G agarose and incubated with 5 µg of antibody per aliquot, unless stated, of RNA Pol II, 1 µg per aliquot, Millipore; PXR (Santa Cruz Biotechnology, Inc.); HNF-4α (Santa Cruz Biotechnology, Inc.); or STAT5 (Santa Cruz Biotechnology, Inc.), overnight at 4°C. Separate aliquots of sample chromatin were incubated with the same amount, and same host species of normal IgG, Millipore, to determine non-specific binding. Protein A/G agarose beads (Santa Cruz Biotechnology, Inc.), were used to collect antibody, antigen and associated chromatin. Beads were washed and then eluted with SDS buffer. Antibody collected chromatin and sample inputs were heated to 65°C to reverse cross links. Proteinase K, purchased from Bio Basic (Markham, ON, Canada), was added for 1 h at 45°C and then DNA was extracted and precipitated prior to being reconstituted in Tris-EDTA buffer. Primers were designed, using NCBI primer-blast, to amplify 100–200 bp regions of genomic DNA around known or putative binding sites of proteins of interest in the promoter region of CYP2C11 or CYP3A2. Real-time PCR was used to quantify RNA Pol II, PXR, HNF-4α and STAT5 promoter region binding.

Data analysis

Results are expressed as mean ± SEM. All statistical analysis was performed using GraphPad Prism (version 5.0; GraphPad Software, Inc., La Jolla, CA, USA). A Michaelis–Menten model was used to fit the formation of testosterone and midazolam metabolites. Statistical differences between control and treated rats were assessed by one-way ANOVA followed by Tukey's *post hoc* test. $P < 0.05$ was considered significant.

Replicates were used in experimental assays to confirm the accuracy of single values. These single value averages were used as individual averages to comprise each *n* value for each of the eight values in each treatment group. Western blots and metabolism assays were performed in duplicate to determine an accurate value for each *n* value. Quantitative PCR results, used for mRNA expression analysis and ChIP, were performed in triplicate for each *n* value.

Materials

Adenine was obtained from Amresco (Solon, OH, USA). Testosterone, 6βOH-testosterone and 16αOH-testosterone were purchased from Steraloids, Inc. (Newport, RI, USA). Carbamazepine and flurazepam were purchased from Cerilliant (Round Rock, TX, USA). Epoetin alfa (EPREX®) was obtained from Janssen-Ortho (Markham, ON, Canada). Midazolam and 1-hydroxymidazolam were purchased from Toronto Research Chemicals, Inc. (Toronto, ON, Canada).

Results

Plasma biochemistry and body weight

Haematocrit was significantly increased in the EPO and CKD EPO groups ($P < 0.001$), and significantly decreased in the CKD group ($P < 0.01$) relative to control. Plasma creatinine levels were 931 and 845% of control in CKD and CKD EPO respectively ($P < 0.001$; Table 1). CKD and CKD EPO groups had plasma urea concentrations 1079 and 713% of control respectively ($P < 0.001$). Plasma liver enzymes AST and ALT were measured to demonstrate adenine diets, and EPO injections did not cause hepatocellular injury (Table 1). Plasma liver enzyme levels in our study were within reference limits and comparable with previously published reports based on gender and body weight (Zhang *et al.*, 2004). Additionally, examination using H&E staining showed normal liver histology in all treatment groups (Figure 1). Kidney damage shown

Table 1

Physical characteristics and biochemistry of control, EPO, CKD and CKD EPO rats

	Control (n = 8)	EPO (n = 8)	CKD (n = 8)	CKD EPO (n = 8)
Body weight (g)	248.5 ± 8.2	249.0 ± 9.7	223.3 ± 18.1	232.6 ± 11.7
Haematocrit (%)	47.2 ± 0.5	67.3 ± 0.7***	36.7 ± 2.3**†††	65.9 ± 2.3***
Plasma creatinine (μmol·L^{-1})	21.4 ± 1.3	25.9 ± 0.6	199.3 ± 24.4***†††	180.8 ± 18.2***†††
Plasma urea (mmol·L^{-1})	6.7 ± 0.4	7.8 ± 0.7	72.3 ± 13.2***†††	47.8 ± 2.5***††
AST (U·L^{-1})	99.6 ± 11.1	87.3 ± 8.1	69.1 ± 8.7	61.3 ± 5.1*
ALT (U·L^{-1})	33.1 ± 2.1	33.0 ± 1.9	8.1 ± 2.2***	8.1 ± 2.2***
Hepatic total P450 content (nmol·mg protein^{-1})	0.71 ± 0.05	0.65 ± 0.07	0.35 ± 0.03***†††	0.35 ± 0.04***†††

Data presented are mean ± SEM. *P < 0.05 relative to control. **P < 0.01 relative to control. ***P < 0.001 relative to control. †P < 0.05 relative to EPO. ††P < 0.01 relative to EPO. †††P < 0.001 relative to EPO.

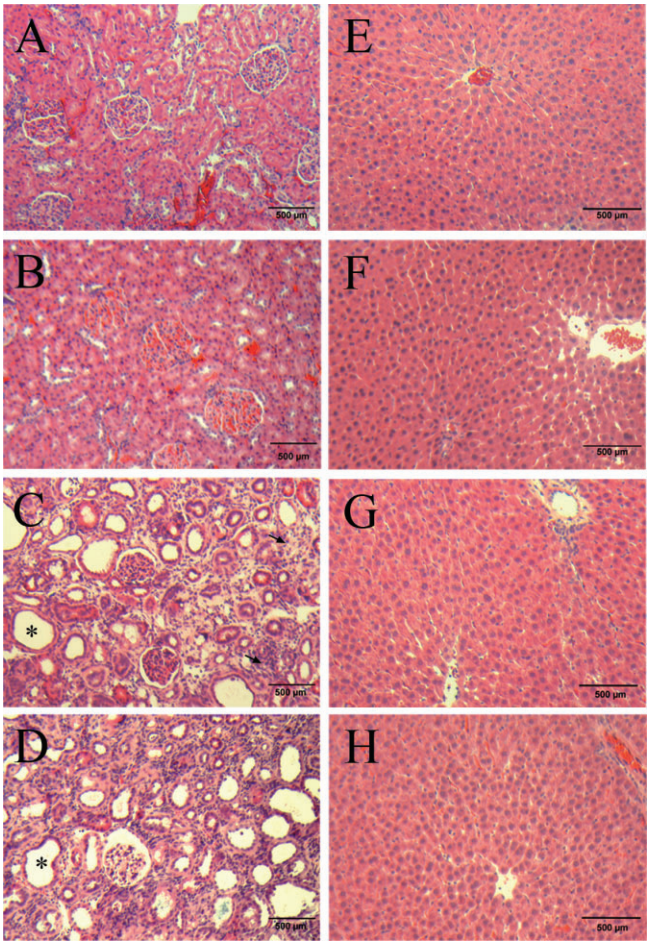

Figure 1

Histology using H&E staining of kidney (A–D) and liver (E–H) tissue from control (A and E), EPO- (B and F), CKD- (C and G) and CKD EPO- (D and H) treated rats. Asterisks (*) mark enlarged nephrons with atrophy of associated tubular cells. Arrows point to increased interstitial cell nuclei, a characteristic of kidney damage. Liver histology of all groups is consistent with normal hepatic structure.

by histology demonstrates damaged, enlarged renal tubules and increased interstitial cell nuclei consistent with previous characterization of the adenine-fed model of kidney disease (Figure 1; Diwan *et al.*, 2013). No histological differences were observed in the liver of EPO, CKD or CKD EPO groups relative to control.

Spectral analysis of total P450 content in liver microsomes showed no decrease between control and EPO-treated groups. Consistent with the 5/6 nephrectomy rat model of CKD used previously (Leblond *et al.*, 2001), a 52% decrease in hepatic total P450 content was demonstrated in CKD and CKD EPO rats relative to control (P < 0.001; Table 1). There were no significant differences in body weight between groups.

Nuclear receptor mRNA expression

CKD EPO rats showed a 49% decrease in CAR hepatic mRNA expression compared with control (P < 0.05; Figure 2). CKD and CKD EPO rat groups had a, 48 and 41% decrease, in PXR hepatic mRNA expression respectively (P < 0.01; Figure 2). There were no significant differences in the hepatic mRNA expression of AhR (P = 0.24), RXRα (P = 0.10) or HNF-4α (P = 0.26) between treatment groups and control.

CYP1A, CYP2C11, CYP2D1 and CYP3A2 mRNA and protein expression

CYP2C11 mRNA expression was decreased by 97 and 98% for CKD and CKD EPO rats, respectively, relative to control (P < 0.001; Figure 3B). Similarly, hepatic CYP3A2 mRNA expression was significantly decreased, relative to control, by 98 and 99% in CKD and CKD EPO rats respectively. Hepatic CYP3A2 mRNA expression was also decreased by 55% in EPO-treated rats compared with control (P < 0.05; Figure 3D). CYP2C11 mRNA expression was not different between control and EPO groups (P = 0.58). No differences were seen in hepatic CYP1A (P = 0.94; Figure 3A) or CYP2D1 (P = 0.46) mRNA expression relative to control.

Similar to mRNA expression, hepatic protein expression of CYP2C11 was significantly decreased by 93 and 96% in the CKD and CKD EPO groups relative to control (P < 0.001; Figure 4B). Hepatic CYP3A2 protein expression was significantly decreased by 79, 98 and 98% in the EPO, CKD and

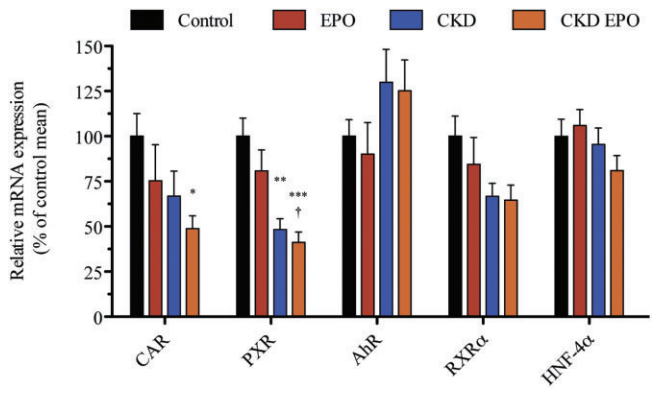

Figure 2

mRNA expression of hepatic nuclear receptors CAR, PXR, AhR, RXRα and HNF-4α. Expression is normalized to housekeeping gene β-actin and shown as relative to percentage of mean control expression for treatment groups EPO CKD and CKD EPO Results shown are mean ± SEM, n = 8. *P < 0.05, **P < 0.01, ***P < 0.001 compared with control; †P < 0.05 compared with EPO.

CKD EPO groups, respectively, relative to control (P < 0.001; Figure 4D). CYP2C11 protein expression was not different between EPO and control groups (P = 0.56). No statistical differences were seen for CYP1A (P = 0.70; Figure 4A) or CYP2D (P = 0.65; Figure 4C) protein expression relative to control.

Hepatic CYP2C11 and CYP3A-mediated drug metabolism

We evaluated the function of CYP2C11, using testosterone and CYP3A, using testosterone and midazolam, in rat liver microsomes. Testosterone is specifically metabolized to 16αOH-testosterone by CYP2C11. Formation of 16αOH-testosterone by CYP2C11 in CKD and CKD EPO rat liver microsome samples was below the limit of detection for most substrate concentrations; therefore, Michaelis–Menten values could not be calculated and statistical analysis could not be performed for the CKD and CKD EPO groups. There was no difference in the V_{max} for the formation of 16αOH-testosterone between EPO and control rat groups (P = 0.61). CYP2C11 V_{max} was substantially higher in control and EPO groups, 1880.8 ± 241.6 and 1669.2 ± 317.9 pmol·min^{-1}·mg·protein^{-1}, respectively, than the unquantifiable metabolite formation in CKD and CKD EPO groups (Figure 5A).

The formation of 6βOH-testosterone and 1-hydroxymidazolam are largely catalysed by CYP3A enzymes. EPO V_{max} for CYP3A-mediated formation of 6βOH-testosterone was significantly decreased by 32% relative to control (P < 0.05; Table 2). Further significant decreases in V_{max} of 51 and 61% were seen in CKD and CKD EPO rats, respectively, compared with controls (P < 0.01; Figure 5B). Maximal enzyme velocity for the formation of 1-hydroxymidazolam was significantly decreased by 71 and 76% in CKD and CKD EPO groups, relative to control respectively (P < 0.01; Figure 5C). EPO V_{max} for the formation of 1-hydroxymidazolam was decreased by 24%, but did not reach statistical significance (P = 0.24). Michaelis–Menten values for the formation of 16αOH-testosterone, 6βOH-testosterone and 1-hydroxymidazolam are summarized in Table 2.

Chromatin immunoprecipitation of RNA Pol II, PXR, HNF-4α

To explore the effects of EPO and CKD on transcriptional regulation of CYP2C11 and CYP3A2, ChIP and quantitative real-time PCR was utilized to quantify binding of RNA Pol II and nuclear receptors, HNF-4α and PXR, to the promoter region of genes. RNA Pol II recruitment to the promoter region of CYP2C11 was decreased by 72 and 78%, relative to control, in CKD and CKD EPO groups respectively (P < 0.05; Figure 6A). Similarly, RNA Pol II binding to the promoter of CYP3A2 was decreased by 88 and 90% in CKD and CKD EPO groups, respectively, compared with control (P < 0.001; Figure 7A). Additionally, RNA Pol II binding to the CYP3A2 promoter was decreased by 52% in the EPO group relative to control (P < 0.01; Figure 7A).

HNF-4α binding to the promoter region of both CYP2C11 and CYP3A2 was also assessed using ChIP. There was a 54 and 56% decrease in HNF-4α binding in the promoter region of CYP2C11 for CKD and CKD EPO groups, respectively, but this failed to reach significance (Figure 6B). In contrast, significant decreases in HNF-4α binding were seen in the promoter region of CYP3A2 with decreases in HNF-4α binding by 62, 71 and 90%, relative to control, in the EPO, CKD and CKD EPO treatment groups respectively (P < 0.05; Figure 7B). Additionally, PXR binding to the CYP3A2 promoter showed 71, 88 and 90% decreased binding, relative to control, in EPO, CKD and CKD EPO groups respectively (P < 0.001; Figure 7C).

Discussion and conclusions

Several earlier reports have described the decreased hepatic expression and function of CYP2C11 and CYP3A2 in rats with CKD using the 5/6 nephrectomy or ligation models of disease (Leblond *et al.*, 2000; 2001; Guevin *et al.*, 2002; Velenosi *et al.*, 2012). To our knowledge, this is the first study to use the adenine-fed model of CKD to study the effects of renal failure on drug metabolism. The 5/6 nephrectomy is the best characterized rodent model of CKD. Despite its widespread utility, the 5/6 nephrectomy models the consequence of CKD (i.e. nephron loss), but does not completely mimic the progression of CKD. The adenine-fed CKD model was used in this study for several reasons: (i) it is a less invasive model with lower rates of mortality; (ii) there is lower variability in creatinine and urea; and (iii) it produces pathological changes that are consistent with progressive CKD (Terai *et al.*, 2008; Hewitson *et al.*, 2009; Diwan *et al.*, 2013). To ensure that the adenine diet model did not also mediate liver toxicity, we confirmed that adenine-fed rats had normal liver histology. In addition, plasma biochemistry results support that the adenine-fed model of CKD and the dosing of EPO do not alter the morphology or affect the integrity of liver tissue.

Our first objective was to confirm that the changes in drug-metabolizing enzyme expression and function in the adenine-fed model of CKD were consistent with the 5/6

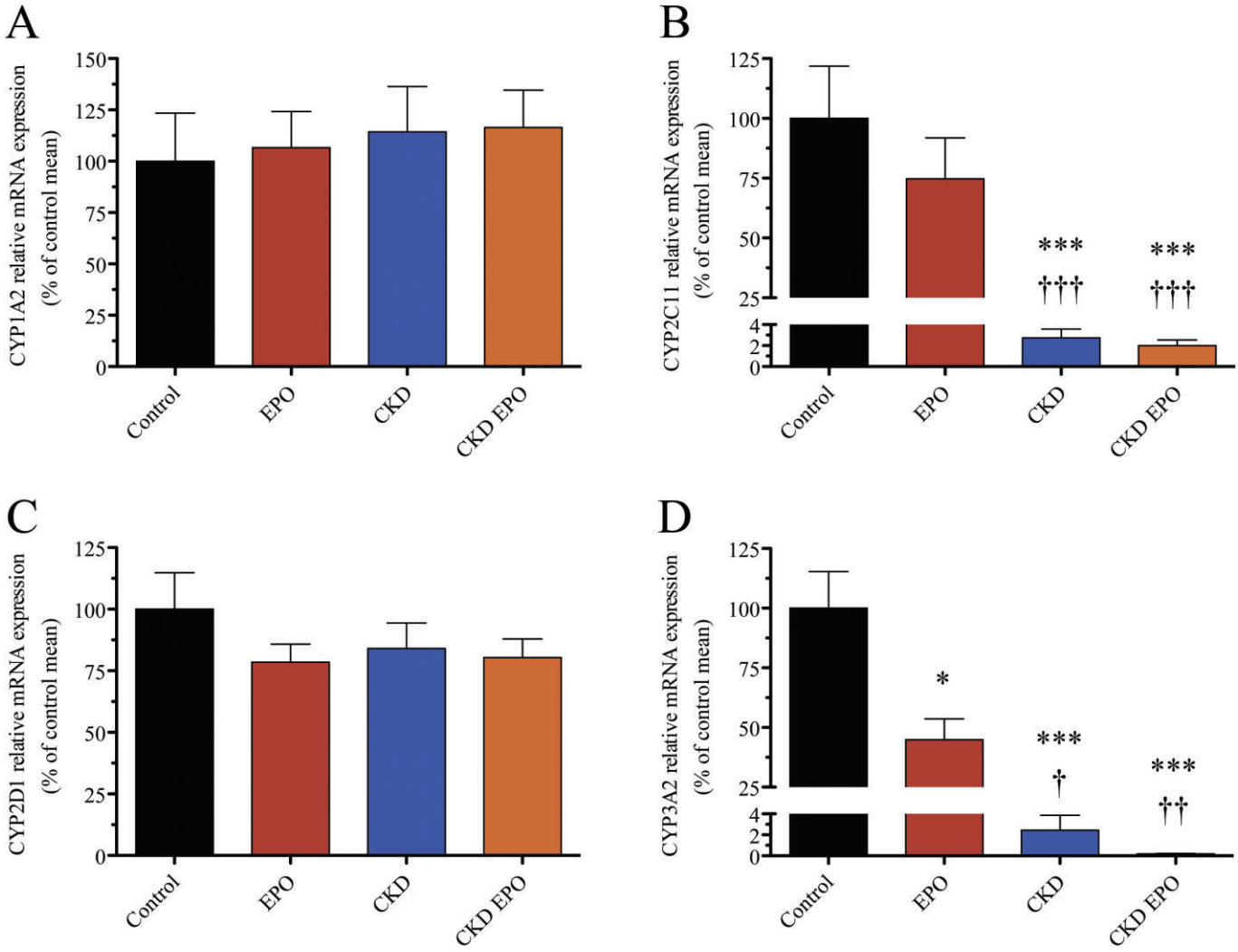

Figure 3

mRNA expression of hepatic CYP1A2 (A), CYP2C11 (B), CYP2D1 (C) and CYP3A2 (D) in control, EPO-, CKD- and CKD EPO-treated rats. Expression is normalized to β-actin and shown as a percentage of control means. Results are mean ± SEM, $n = 8$. *$P < 0.05$, **$P < 0.01$, ***$P < 0.001$, compared with control; †$P < 0.05$, ††$P < 0.01$, †††$P < 0.001$ compared with EPO.

nephrectomy model. Our data clearly demonstrate that the adenine-fed model of CKD causes pronounced decreases of hepatic CYP2C11 and CYP3A2 expression and function, consistent with previously published work using the 5/6 nephrectomy model of CKD (Leblond *et al.*, 2001; Guevin *et al.*, 2002; Velenosi *et al.*, 2012). Our next objective was to evaluate our hypothesis that EPO would partially restore expression of P450s down-regulated by CKD. We hypothesized EPO would restore P450 expression in CKD for two reasons. First, recent findings demonstrate that EPO is able to activate nuclear receptors known to be involved in the regulation of drug transport proteins involved in drug disposition (Naik *et al.*, 2006; Lu *et al.*, 2010; Meyer Zu Schwabedissen *et al.*, 2010). Second, induction of CYP3A6, the rabbit orthologue of human CYP3A4, was observed in a hypoxia study using isolated rabbit hepatocytes. The authors showed the involvement of plasma mediators (Fradette *et al.*, 2002) and convincingly showed, using anti-EPO antibodies, that part of the CYP3A6 induction observed was due to the actions of EPO (Fradette *et al.*, 2002). Despite these previous findings and contrary to our hypothesis, we observed no restoration in CKD-mediated down-regulation of P450 enzymes. In fact, our results demonstrate that 2 weeks of IP EPO injections significantly decreases CYP3A2 mRNA expression, leading to a corresponding decrease in protein expression and metabolism of the CYP3A probe substrate testosterone. Although significant decreases were seen in mRNA and protein expression of CYP3A2, the metabolism of probe substrates did not demonstrate the same degree of difference between control and EPO-treated rats. This result is likely to be due to the actions of other P450 enzymes able to metabolize testosterone and midazolam to the metabolites, 6βOH-testosterone and 1OH-midazolam respectively (Chovan *et al.*, 2007). Previous work by Chovan *et al.* (2007) has reported that, for the hydroxylation of midazolam in rat liver microsomes, only 32% of metabolite formation is achieved by CYP3A2. Other P450

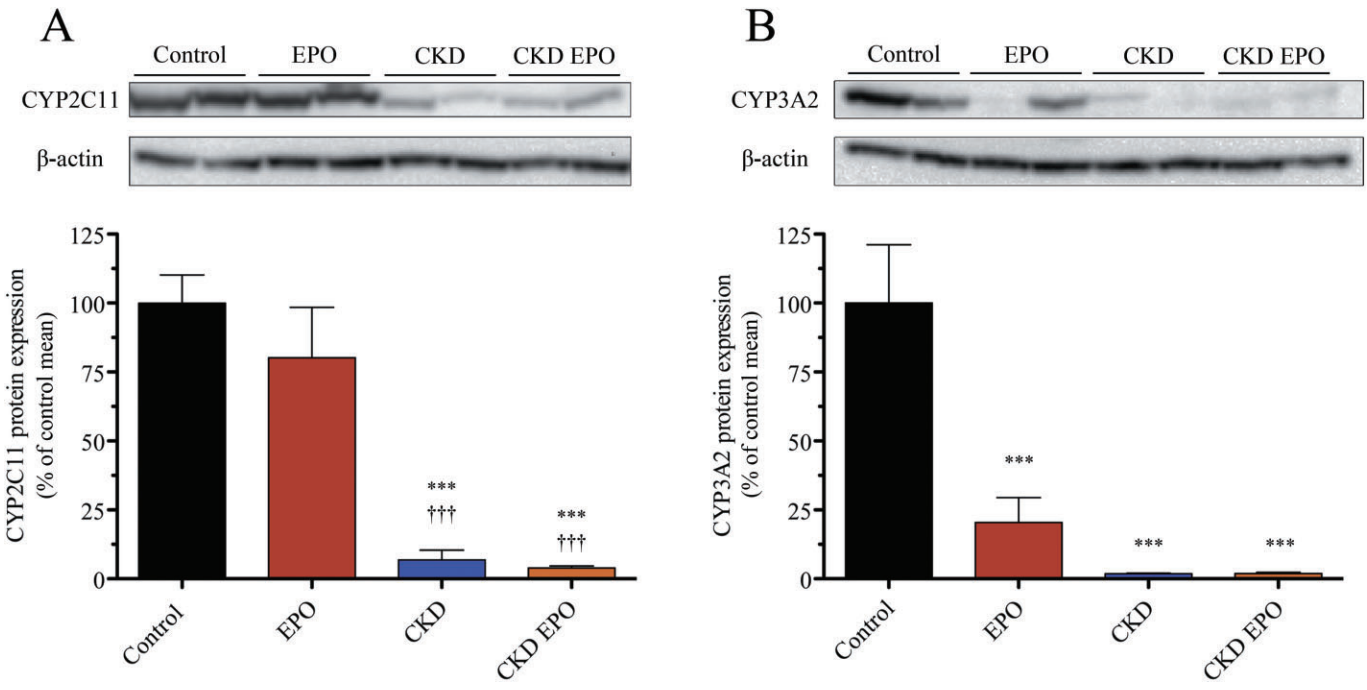

Figure 4

Protein expression of hepatic CYP1A (A), CYP2C11 (B), CYP2D (C) and CYP3A2 (D) in control, EPO-, CKD- and CKD EPO-treated rats. Protein bands are standardized to β-actin and expressed as relative densitometry units with the average of control bands arbitrarily defined as 100%. Results shown are mean ± SEM, $n = 8$. ***$P < 0.001$ compared with control; $^{\dagger\dagger\dagger}P < 0.001$ compared with EPO.

isozymes, such as CYP2C11 and CYP2C13 are also involved. In addition, the formation of 6βOH-testosterone is also accomplished by the activity of CYP2A2, CYP1A1 and others (Chovan *et al.*, 2007). Finally, both testosterone and midazolam are metabolized by CYP3A1 and its hepatic expression was not evaluated in the current study. Further, we demonstrate that treatment with EPO decreases PXR and HNF-4α binding to the CYP3A2 promoter and that this decrease in binding is concurrent with a decrease in RNA polymerase II binding. Although EPO has been shown to activate other nuclear receptors, such as LXR, our data demonstrate that it mediates decreased activity of hepatic PXR and HNF-4α. Despite the widespread use of rodent models for the study of CKD and hypoxia-induced changes in P450 expression, some differences in regulation, relative to the human, have been described. For example, although human and rodent PXR share a high sequence homology and similar target genes, interspecies differences in ligand-dependent activation exist (Watkins *et al.*, 1985; Wrighton *et al.*, 1985). Accordingly, the differences we observed in nuclear receptor binding in our rat study need to be confirmed in a humanized system (e.g. humanized mouse models).

EPO treatment is targeted at increasing the proliferation and differentiation of erythrocytes in order to treat anaemia. Erythropoiesis requires iron, for haeme synthesis, as the prosthetic haeme group is required for the formation of haemoglobin. As P450 drug-metabolizing enzymes are also haemoproteins, one potential explanation of our data is that EPO administration simply depletes or limits the iron or haeme pool. The consequence of a depleted haeme pool would be a decrease in total P450 content with an increase in cytochrome P420. We found no significant difference in hepatic total P450 content between control and EPO-treated groups indicating that EPO itself does not simply decrease the iron or haem pool available for P450 synthesis. A significant decrease in total hepatic P450 content was observed in CKD and CKD EPO groups; however, this finding was expected and is consistent with previous studies using the 5/6 nephrectomy model of CKD (Leblond *et al.*, 2000). Iron deficiency is known to significantly decrease plasma iron, total liver iron and liver ferritin (Dhur *et al.*, 1989). However, iron deficiency has been shown in many studies to not affect total hepatic microsomal protein or P450 content (Catz *et al.*, 1970; Dhur *et al.*, 1989). Further, limiting haeme has only been shown to decrease P450 induction by phenobarbital, not basal expression, in knockout mice unable to synthesize haem (Jover *et al.*, 2000). Additionally, the rats in our study were not subject to iron restriction; thus, it is unlikely that changes in P450 protein content were influenced by utilization of iron for erythropoiesis. Although we did not measure iron in our study, a previous study in rats with CKD receiving EPO did not display any changes in serum iron concentration (Srai *et al.*, 2010).

Previous reports demonstrate an up-regulation of hepatic CYP3A6 in rabbits exposed to hypoxia (Kurdi *et al.*, 1999; Fradette *et al.*, 2002). One of the primary consequences of hypoxia is the stabilization of hypoxia-inducible factor (HIF) α subunits. HIF-1α and HIF-2α heterodimerize with HIF-1β and bind to HIF-responsive elements in target genes such as EPO to up-regulate their transcription. Indeed, increased synthesis of EPO is consistently observed in hypoxic conditions.

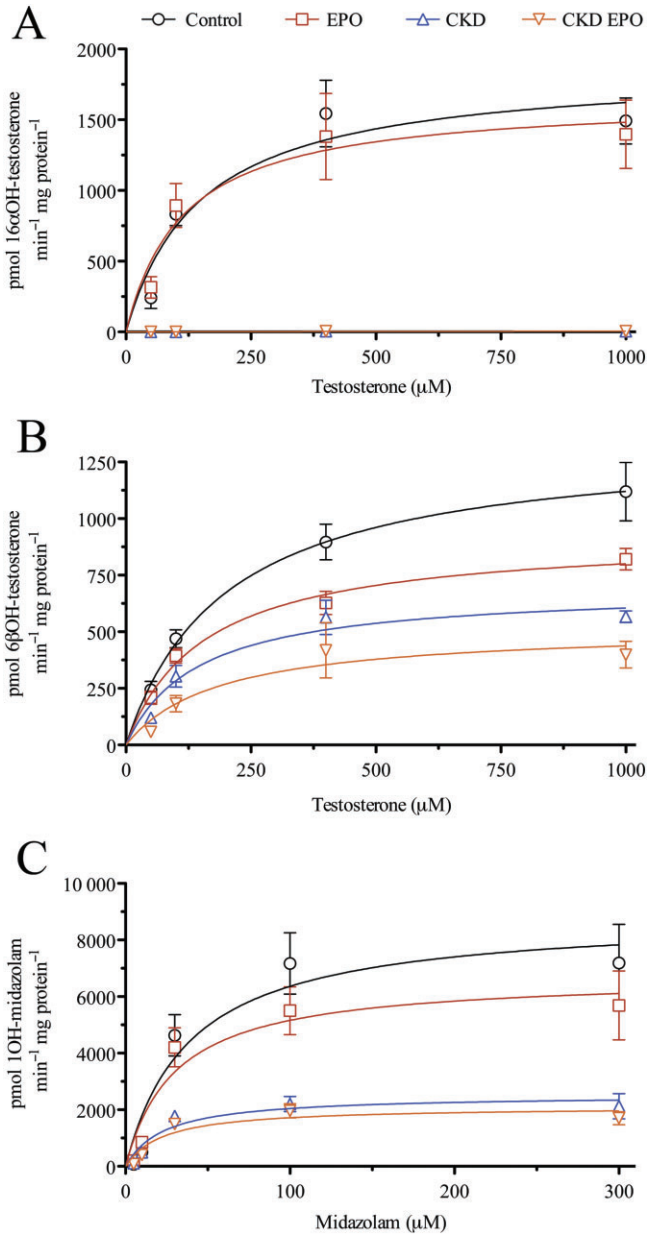

Figure 5

Michaelis–Menten plots of the formation of 16αOH-testosterone (A), 6βOH-testosterone (B) and 1OH-midazolam (C) after incubation of rat liver microsomes with 1 mM NADPH and substrate concentrations of 50, 100, 400 and 1000 μM for testosterone and 5, 10, 30, 100 and 300 μM for midazolam. Formation of 16αOH-testosterone in CKD and CKD EPO liver microsomes was at or below the limit of detection for most concentrations. Results are presented as mean ± SEM, $n = 8$.

Fradette *et al.* (2002) elegantly demonstrate that anti-EPO antibodies partially abrogate the induction of CYP3A6 under hypoxic conditions. Although our data appear to contradict this finding, it must be noted that there are marked species differences in the transcriptional regulation of P450s, and our study did not directly investigate the effect of hypoxia. Consistent with our observations, the expression and function of drug-metabolizing enzymes, including CYP3A4, are decreased after exposure to hypoxia in differentiated human HepaRG cells (Legendre *et al.*, 2009). In that study, hypoxia-mediated down-regulation of CYP3A4 was shown to involve HIF-1α. Although implicated in the down-regulation of CYP3A, HIF-1α involvement in that study was thought to be acting by an indirect, and unknown, mechanism (Legendre *et al.*, 2009). Despite being an *in vitro* experiment using a hepatic cell line, it is possible that this unknown mechanism involves EPO signalling. Hypoxia, caused by low oxygen tension or anaemia secondary to bilateral nephrectomy or haemorrhage, has been previously shown to increase hepatic EPO production (Fried, 1972; Bondurant and Koury, 1986).

Based on the previous work by Legendre *et al.* (2009) on the effect of hypoxia on CYP3A4 in HepaRG cells, our data suggest that EPO could be the next step in the elusive mechanism that links hypoxia and HIF activation to decreased CYP3A expression. Although constitutively expressed, HIF-1α subunits are extremely sensitive to oxygen and, in the presence of oxygen, are hydroxylated, recognized for ubiquitination and subsequently proteosomally degraded (Jaakkola *et al.*, 2001). Conversely, under hypoxic conditions HIF-1α and HIF-2α act as transcription factors to activate many genes including activating the transcription of EPO as shown in states of low oxygen tension (Lacombe *et al.*, 1988; Wang and Semenza, 1993). The relationship between HIFs and EPO, and corresponding evidence of decreases in CYP3A4 and CYP3A2, respectively, suggests that EPO is largely responsible for hypoxia-mediated changes in the expression of CYP3A. Our data support that exposure to EPO causes decreased binding of PXR, HNF-4α and RNA polymerase II to the promoter region of CYP3A2. It remains to be determined whether the effect of EPO on CYP3A expression is a direct result of EPO signalling or are a consequence of changes in the expression of other genes mediated by EPO. Interestingly, EPO did not alter the expression of, or the transcription factor binding to the promoter region of CYP2C11. Although the regulation of these enzymes has notable differences, they are both regulated to some degree by HNF-4α. This suggests that the mechanism of EPO-mediated down-regulation of CYP3A2 may target other currently unknown factors specific to regulation of CYP3A2 that are not involved in the regulation of CYP2C11.

The EPO receptor is expressed on many non-haematopoietic tissues including liver. Upon ligand binding, EPO can activate three major intracellular signalling pathways: (i) the JAK2; (ii) the ERK; and (iii) the PI3K/Akt pathways. Activation of the JAK2 pathway activates STAT5 by phosphorylation (Gouilleux *et al.*, 1995; Parganas *et al.*, 1998). Phosphorylated STAT5 is able to enter the nucleus and act as a transcription factor in the promoter region of genes both as an activator and a suppressor of transcription (John *et al.*, 1999). We attempted to characterize STAT5 binding to putative sites in the CYP3A promoter, but have been unable to confirm binding to these sites (data not shown). Activation of the ERK1/2 pathway has been shown to interact with phosphorylated CAR, preventing its dephosphorylation and retaining it in the cytoplasm (Osabe and Negishi, 2011). PXR translocation to the nucleus is also decreased by phosphorylation (Lichti-Kaiser *et al.*, 2009). Therefore, it is possible that EPO-induced ERK activation plays a role in retaining

Table 2

Michaelis-Menten kinetic values for formation of 16α-OH testosterone (CYP2C11), 6β-OH testosterone (CYP3A) and 1-OH midazolam (CYP3A) in control, EPO, CKD and CKD EPO rat liver microsomes

	16α-OH testosterone		6β-OH testosterone		1-OH midazolam	
	K_m	V_{max}	K_m	V_{max}	K_m	V_{max}
	μM	pmol·min^{-1}·mg·protein^{-1}	μM	pmol·min^{-1}·mg·protein^{-1}	μM	pmol·min^{-1}·mg·protein^{-1}
Control	148 ± 23	1881 ± 242	202 ± 28	1369 ± 179	39 ± 5	9025 ± 1645
EPO	122 ± 16	1669 ± 318	159 ± 19	926 ± 56*	30 ± 6	6932 ± 1476
CKD	n/d	n/d	155 ± 24	700 ± 52**	24 ± 4*	2591 ± 487**
CKD EPO	n/d	n/d	225 ± 48	543 ± 105***	22 ± 3*	2127 ± 283**

Data presented are mean ± SEM. n/d, not detectable. *P < 0.05 relative to control. **P < 0.01 relative to control. ***P < 0.001 relative to control.

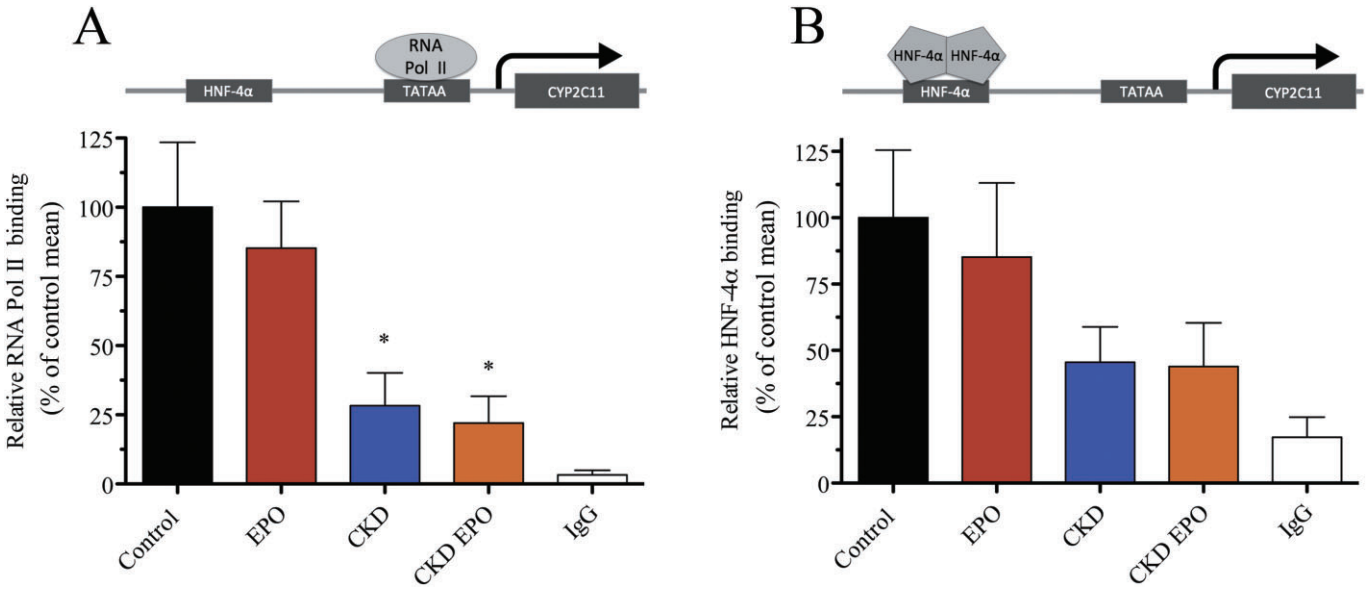

Figure 6

ChIP in hepatic tissue to quantify the binding of RNA pol II (A) and HNF-4α binding (B) to the promoter region of CYP2C11 for control, EPO (red), CKD and CKD EPO rats. Results are standardized to input DNA and expressed as a percentage of mean control value. Samples immunoprecipitated with normal mouse IgG (A) or rabbit IgG (B) are shown as IgG (white). Results are mean ± SEM, n = 8. *P < 0.05 relative to control.

nuclear receptors in the cytoplasm and therefore decreasing CYP3A2 transcription. The last cell signalling pathway activated by EPO is the PI3K/Akt pathway. Previous studies have shown that downstream kinases in this pathway phosphorylate and negatively regulate the transcriptional activity of PXR (Lichti-Kaiser *et al.*, 2009; Pondugula *et al.*, 2009). Finally, a recent study has shown that EPO activates the LXR in macrophages (Lu *et al.*, 2010). The LXR has been shown to transcriptionally repress the activity of both PXR and CAR, which provides another potential explanation of the molecular mechanism linking EPO to decreased CYP3A2 expression in our study (Handschin *et al.*, 2002; Pondugula *et al.*, 2009). It is clear that EPO mediates its non-haematopoietic effects via many distinct molecular pathways and that further work is needed to isolate the specific mechanism associated with EPO-induced decreases in nuclear receptor binding and CYP3A expression.

In conclusion, this study demonstrates that EPO decreases the expression and function of hepatic CYP3A2 by decreasing the binding of the nuclear receptors PXR and HNF-4α. To our knowledge, this is the first study that has evaluated the effect of EPO on drug metabolism. As the principal enzyme for the metabolism of many drugs, knowledge of the effects of EPO on CYP3A expression and function are important for patient safety and appropriate drug dosing. Greater understanding on how EPO affects hepatic P450 expression *in vitro* and

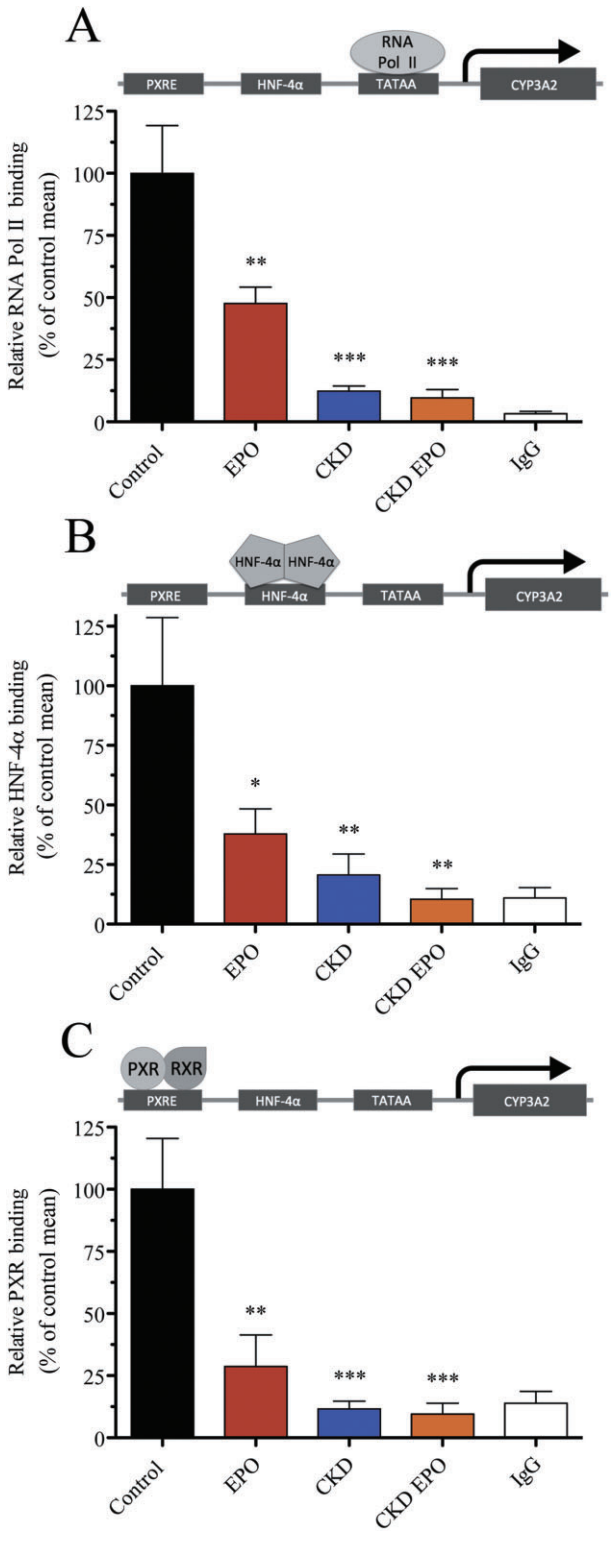

Figure 7

ChIP in hepatic tissue to quantify the binding of RNA pol II (A), HNF-4α binding (B) and PXR (C) to the promoter region of CYP3A2 for control, EPO, CKD and CKD EPO rats. Results are standardized to input DNA and expressed as a percentage of mean control value. Samples immunoprecipitated with normal mouse IgG (A) or rabbit IgG (B and C) are shown as IgG. Results are mean ± SEM, $n = 8$. *$P < 0.05$, **$P < 0.01$, ***$P < 0.001$, compared with control.

in vivo, will be needed before evaluating the pharmacokinetics of individual drugs to optimize drug dosing in patients receiving recombinant human EPO.

Acknowledgements

This study was made possible by funding from the Natural Sciences and Engineering Research Council of Canada (NSERC) the University of Western Ontario Academic Development Fund and the Canadian Foundation for Innovation. We would like to thank Dr Daniel B. Hardy for his procedural assistance and protocol for chromatin immunoprecipitation experiments.

Author contributions

All authors contributed to the experimental design and data and statistical analyses. All experiments were conducted by D. A. F. with T. J. V. for all rat procedures and UPLC operation. Reagents and analytical tools were contributed by B. L. U. The manuscript was drafted by D. A. F., with additions and revisions by all authors.

Conflict of interest

None.

References

Alexander SPH, Benson HE, Faccenda E, Pawson AJ, Sharman JL, Spedding M *et al.* (2013a). The Concise Guide to PHARMACOLOGY 2013/14: Enzymes. Br J Pharmacol 170: 1797–1867.

Alexander SPH, Benson HE, Faccenda E, Pawson AJ, Sharman JL, Spedding M *et al.* (2013b). The Concise Guide to PHARMACOLOGY 2013/14: Nuclear Hormone Receptors. Br J Pharmacol 170: 1652–1675.

Bondurant MC, Koury MJ (1986). Anemia induces accumulation of erythropoietin mRNA in the kidney and liver. Mol Cell Biol 6: 2731–2733.

Catz CS, Juchau MR, Yaffe SJ (1970). Effects of iron, riboflavin and iodide deficiencies on hepatic drug-metabolizing enzyme systems. J Pharmacol Exp Ther 174: 197–205.

Chovan JP, Ring SC, Yu E, Baldino JP (2007). Cytochrome P450 probe substrate metabolism kinetics in Sprague Dawley rats. Xenobiotica 37: 459–473.

Dhur A, Galan P, Hercberg S (1989). Effects of different degrees of iron deficiency on cytochrome P450 complex and pentose phosphate pathway dehydrogenases in the rat. J Nutr 119: 40–47.

Diwan V, Mistry A, Gobe G, Brown L (2013). Adenine-induced chronic kidney and cardiovascular damage in rats. J Pharmacol Toxicol Methods 68: 197–207.

Eschbach JW (2002). Anemia management in chronic kidney disease: role of factors affecting epoetin responsiveness. J Am Soc Nephrol 13: 1412–1414.

Food and Drug Administration (FDA) (2010). Pharmacokinetics in patients with impaired renal function – study design, data analysis, and impact on dosing and labeling.

Fradette C, Bleau AM, Pichette V, Chauret N, Du Souich P (2002). Hypoxia-induced down-regulation of CYP1A1/1A2 and up-regulation of CYP3A6 involves serum mediators. Br J Pharmacol 137: 881–891.

Fried W (1972). The liver as a source of extrarenal erythropoietin production. Blood 40: 671–677.

Gouilleux F, Pallard C, Dusanter-Fourt I, Wakao H, Haldosen LA, Norstedt G *et al*. (1995). Prolactin, growth hormone, erythropoietin and granulocyte-macrophage colony stimulating factor induce MGF-Stat5 DNA binding activity. EMBO J 14: 2005–2013.

Guevin C, Michaud J, Naud J, Leblond FA, Pichette V (2002). Down-regulation of hepatic cytochrome p450 in chronic renal failure: role of uremic mediators. Br J Pharmacol 137: 1039–1046.

Handschin C, Podvinec M, Amherd R, Looser R, Ourlin JC, Meyer UA (2002). Cholesterol and bile acids regulate xenosensor signaling in drug-mediated induction of cytochromes P450. J Biol Chem 277: 29561–29567.

Hewitson TD, Ono T, Becker GJ (2009). Small animal models of kidney disease: a review. Methods Mol Biol 466: 41–57.

Ibeanu GC, Goldstein JA (1995). Transcriptional regulation of human CYP2C genes: functional comparison of CYP2C9 and CYP2C18 promoter regions. Biochemistry 34: 8028–8036.

Jaakkola P, Mole DR, Tian YM, Wilson MI, Gielbert J, Gaskell SJ *et al*. (2001). Targeting of HIF-alpha to the von Hippel–Lindau ubiquitylation complex by O2-regulated prolyl hydroxylation. Science 292: 468–472.

John S, Vinkemeier U, Soldaini E, Darnell JE Jr, Leonard WJ (1999). The significance of tetramerization in promoter recruitment by Stat5. Mol Cell Biol 19: 1910–1918.

Jover R, Hoffmann F, Scheffler-Koch V, Lindberg RL (2000). Limited heme synthesis in porphobilinogen deaminase-deficient mice impairs transcriptional activation of specific cytochrome P450 genes by phenobarbital. Eur J Biochem 267: 7128–7137.

Kilkenny C, Browne W, Cuthill IC, Emerson M, Altman DG (2010). Animal research: reporting *in vivo* experiments: the ARRIVE guidelines. Br J Pharmacol 160: 1577–1579.

Kurdi J, Maurice H, El-Kadi AO, Ong H, Dalkara S, Belanger PM *et al*. (1999). Effect of hypoxia alone or combined with inflammation and 3-methylcholanthrene on hepatic cytochrome P450 in conscious rabbits. Br J Pharmacol 128: 365–373.

Lacombe C, Da Silva JL, Bruneval P, Fournier JG, Wendling F, Casadevall N *et al*. (1988). Peritubular cells are the site of erythropoietin synthesis in the murine hypoxic kidney. J Clin Invest 81: 620–623.

Leblond F, Guevin C, Demers C, Pellerin I, Gascon-Barre M, Pichette V (2001). Downregulation of hepatic cytochrome P450 in chronic renal failure. J Am Soc Nephrol 12: 326–332.

Leblond FA, Giroux L, Villeneuve JP, Pichette V (2000). Decreased *in vivo* metabolism of drugs in chronic renal failure. Drug Metab Dispos 28: 1317–1320.

Legendre C, Hori T, Loyer P, Aninat C, Ishida S, Glaise D *et al*. (2009). Drug-metabolising enzymes are down-regulated by hypoxia in differentiated human hepatoma HepaRG cells: HIF-1alpha involvement in CYP3A4 repression. Eur J Cancer 45: 2882–2892.

Lichti-Kaiser K, Brobst D, Xu C, Staudinger JL (2009). A systematic analysis of predicted phosphorylation sites within the human pregnane X receptor protein. J Pharmacol Exp Ther 331: 65–76.

Livak KJ, Schmittgen TD (2001). Analysis of relative gene expression data using real-time quantitative PCR and the 2(-delta delta C(T) method. Methods 25: 402–408.

Lu KY, Ching LC, Su KH, Yu YB, Kou YR, Hsiao SH *et al*. (2010). Erythropoietin suppresses the formation of macrophage foam cells: role of liver X receptor alpha. Circulation 121: 1828–1837.

Manley HJ, Garvin CG, Drayer DK, Reid GM, Bender WL, Neufeld TK *et al*. (2004). Medication prescribing patterns in ambulatory haemodialysis patients: comparisons of USRDS to a large not-for-profit dialysis provider. Nephrol Dial Transplant 19: 1842–1848.

McGrath J, Drummond G, McLachlan E, Kilkenny C, Wainwright C (2010). Guidelines for reporting experiments involving animals: the ARRIVE guidelines. Br J Pharmacol 160: 1573–1576.

Meyer Zu Schwabedissen HE, Bottcher K, Chaudhry A, Kroemer HK, Schuetz EG, Kim RB (2010). Liver X receptor alpha and farnesoid X receptor are major transcriptional regulators of OATP1B1. Hepatology 52: 1797–1807.

Naik SU, Wang X, Da Silva JS, Jaye M, Macphee CH, Reilly MP *et al*. (2006). Pharmacological activation of liver X receptors promotes reverse cholesterol transport *in vivo*. Circulation 113: 90–97.

Nolin TD, Frye RF, Matzke GR (2003). Hepatic drug metabolism and transport in patients with kidney disease. Am J Kidney Dis 42: 906–925.

Nolin TD, Frye RF, Le P, Sadr H, Naud J, Leblond FA *et al*. (2009). ESRD impairs nonrenal clearance of fexofenadine but not midazolam. J Am Soc Nephrol 20: 2269–2276.

Omura T, Sato R (1964). The carbon monoxide-binding pigment of liver microsomes. I. Evidence for its hemoprotein nature. J Biol Chem 239: 2370–2378.

Osabe M, Negishi M (2011). Active ERK1/2 protein interacts with the phosphorylated nuclear constitutive active/androstane receptor (CAR; NR1I3), repressing dephosphorylation and sequestering CAR in the cytoplasm. J Biol Chem 286: 35763–35769.

Parganas E, Wang D, Stravopodis D, Topham DJ, Marine JC, Teglund S *et al*. (1998). JAK2 is essential for signaling through a variety of cytokine receptors. Cell 93: 385–395.

Pawson AJ, Sharman JL, Benson HE, Faccenda E, Alexander SP, Buneman OP *et al*.; NC-IUPHAR (2014). The IUPHAR/BPS Guide to PHARMACOLOGY: an expert-driven knowledge base of drug targets and their ligands. Nucl. Acids Res 42 (Database Issue): D1098–1106.

Pinto JP, Ribeiro S, Pontes H, Thowfeequ S, Tosh D, Carvalho F *et al*. (2008). Erythropoietin mediates hepcidin expression in hepatocytes through EPOR signaling and regulation of C/EBPalpha. Blood 111: 5727–5733.

Pondugula SR, Dong H, Chen T (2009). Phosphorylation and protein-protein interactions in PXR-mediated CYP3A repression. Expert Opin Drug Metab Toxicol 5: 861–873.

Sohi G, Marchand K, Revesz A, Arany E, Hardy DB (2011). Maternal protein restriction elevates cholesterol in adult rat offspring due to repressive changes in histone modifications at the cholesterol 7alpha-hydroxylase promoter. Mol Endocrinol 25: 785–798.

Srai SK, Chung B, Marks J, Pourvali K, Solanky N, Rapisarda C *et al*. (2010). Erythropoietin regulates intestinal iron absorption in a rat model of chronic renal failure. Kidney Int 78: 660–667.

Talbert RL (1994). Drug dosing in renal insufficiency. J Clin Pharmacol 34: 99–110.

Terai K, Mizukami K, Okada M (2008). Comparison of chronic renal failure rats and modification of the preparation protocol as a hyperphosphataemia model. Nephrology (Carlton) 13: 139–146.

Tirona RG, Lee W, Leake BF, Lan LB, Cline CB, Lamba V *et al.* (2003). The orphan nuclear receptor HNF4alpha determines PXR- and CAR-mediated xenobiotic induction of CYP3A4. Nat Med 9: 220–224.

Velenosi TJ, Urquhart BL (2014). Pharmacokinetic considerations in chronic kidney disease and patients requiring dialysis. Expert Opin Drug Metab Toxicol 10: 1131–1143.

Velenosi TJ, Fu AY, Luo S, Wang H, Urquhart BL (2012). Down-regulation of hepatic CYP3A and CYP2C mediated metabolism in rats with moderate chronic kidney disease. Drug Metab Dispos 40: 1508–1514.

Wang GL, Semenza GL (1993). General involvement of hypoxia-inducible factor 1 in transcriptional response to hypoxia. Proc Natl Acad Sci U S A 90: 4304–4308.

Watkins PB, Wrighton SA, Maurel P, Schuetz EG, Mendez-Picon G, Parker GA *et al.* (1985). Identification of an inducible form of cytochrome P-450 in human liver. Proc Natl Acad Sci U S A 82: 6310–6314.

Wienkers LC, Heath TG (2005). Predicting *in vivo* drug interactions from *in vitro* drug discovery data. Nat Rev Drug Discov 4: 825–833.

Wrighton SA, Schuetz EG, Watkins PB, Maurel P, Barwick J, Bailey BS *et al.* (1985). Demonstration in multiple species of inducible hepatic cytochromes P-450 and their mRNAs related to the glucocorticoid-inducible cytochrome P-450 of the rat. Mol Pharmacol 28: 312–321.

Wrighton SA, VandenBranden M, Ring BJ (1996). The human drug metabolizing cytochromes P450. J Pharmacokinet Biopharm 24: 461–473.

Zanger UM, Schwab M (2013). Cytochrome P450 enzymes in drug metabolism: regulation of gene expression, enzyme activities, and impact of genetic variation. Pharmacol Ther 138(: 103–141.

Zhang ZP, Tian YH, Li R, Cheng XQ, Guo SM, Zhang JX *et al.* (2004). The comparison of the normal blood biochemical values of Wistar rats with different age and sex. Asian J Drug Metab Pharmacokinet 4: 215–218.

Supporting information

Additional Supporting Information may be found in the online version of this article at the publisher's web-site:

http://dx.doi.org/10.1111/bph.12932

Figure S1 Eadie-Hofstee plot of hepatic in vitro CYP3A-mediated microsomal conversion of Testosterone to 6BetaOH-Testosterone by Control (black), EPO (red), CKD (Blue) and CKD EPO (Orange) treated rats. n = 8 for each treatment group.
Table S1 Real-time PCR primers.